

Spectral CUSUM for Online Network Structure Change Detection

Minghe Zhang, Liyan Xie, and Yao Xie^{*}

June 24, 2022

Abstract

Detecting abrupt changes in the community structure of a network from noisy observations is a fundamental problem in statistics and machine learning. This paper presents an online change detection algorithm called Spectral-CUSUM to detect unknown network structure changes through a generalized likelihood ratio statistic. We characterize the average run length (ARL) and the expected detection delay (EDD) of the Spectral-CUSUM procedure and prove its asymptotic optimality. Finally, we demonstrate the good performance of the Spectral-CUSUM procedure and compare it with several baseline methods using simulations and real data examples on seismic event detection using sensor network data.

1 Introduction

Detecting network structure change from sequential data is a fundamental problem in high-dimensional data analysis, emerging from multiple applications, including seismic sensor networks [1], traffic networks [2], swarm behavior monitoring [3], and social network change detection [4]. A community corresponds to a subset of nodes with much higher connectivity within the group than across groups. Real-world communication structure changes can be complicated. In various settings, the change may correspond to the emergence of a community, switching community memberships, changes in the number of communities, etc.

The need for community structure change detection is high for high-dimensional sequential data, which tend to have complex inter-dependent relationships between different dimensions. Such interdependence structure can be explicit, where the network topology be inferred from data. In the network settings *the characteristic of the changes* will be a shift in *structures* of the underlying parameters, which is fundamentally different from a simple mean-shift considered in the change-point detection literature. As been recognized, it is possible to exploit the underlying dependence structures to design asymptotically optimal detection algorithms [5]. In addition, we typically need detection procedure to be computationally and memory efficient, as the data streams in this setting are often very high-dimensional and generated at a high speed.

We first give a few example of detecting changes exploring community structures:

- Seismic sensor networks: The seismic research has been based on the massive amount of continuous data recorded by ultra-dense seismic sensor arrays and many such data are publicly available on IRIS (<https://www.iris.edu>). In the old days, network seismology treats seismic signals individually - one sensor at a time - and detects an earthquake when multiple impulsive arrivals consistent with a source within the Earth

^{*}Minghe Zhang (Email: mzhang388@gatech.edu), and Yao Xie (Email: yao.xie@isye.gatech.edu, corresponding author) are with H. Milton Stewart School of Industrial and Systems Engineering, Georgia Institute of Technology, Atlanta, GA, 30332 USA.

[†]Liyan Xie (Email: xieliyan@cuhk.edu.cn) is with School of Data Science, The Chinese University of Hong Kong, Shenzhen, China.

[6]. Recently, with advances in sensor technology, which bring densely sampled data and high-performance computing and communication, we may be able to use a *network-based detection* by exploiting correlations between sensors to extract coherence signals. This will enhance the systematic detection of weak and unusual events that currently go undetected using individual sensors. Detecting such weak events is very crucial for earthquake prediction [7, 8], oil field exploration, volcano monitoring, and deeper earth studies [9].

- **Social networks:** The widespread use of social networks leads to a large amount of user-generated continuous data, which is quite valuable in studying many social phenomena. One important application is to detect change points using social network data. These change points may represent the collective anticipation of or response to external events or system “shocks” [10]. Detecting such changes can provide a better understanding of patterns of social life. In other cases, early detection of change-point can predict or even prevent social stress due to disease or international threats. In social network data [11], each node represents one individual, and the edge represents the relationship between two individuals.
- **Manifold** is a common low-dimensional structure that lies in high-dimensional data, which can be captured using a similar network such as Isomap and Laplacian Eigenmaps [12]. Thus, change in the manifold structure can be detected from similar graphs.

In this paper, we present a new online change-point detection procedure, the Spectral CUSUM, to detect network structure changes by observing node features. We model the network structure through the inverse covariance of the noisy Gaussian features. Based on such a model, Spectral CUSUM is derived based on generalized likelihood ratios, where the unknown post-change parameters are estimated sequentially. This approach enables us to detect general types of structural changes, including the emergence of community and switching membership. The main theoretical contribution is to show the first-order asymptotic optimality of Spectral CUSUM, and characterizing the optimal choice of the parameters. We also present an online scheme for computing the detection statistic based on subspace tracking that is computationally and memory efficient. We demonstrate the meritorious performance of Spectral CUSUM through simulated and real-data examples of detecting changes in Yellowstone seismic sensors data.

The rest of the paper is organized as follows. Section 2 provides a detailed formulation of the emerging communities problem as well as the switching membership problem. Section 3 introduces the exact-CUSUM and the proposed Spectral-CUSUM procedure. Section 4 presents the asymptotic analysis of the proposed detection scheme together with parameter optimization and proof of the first-order asymptotic optimality. Section 5 presents an efficient gradient-based algorithm to keep track of the underlying community structure. Section 6 gives simulation and real data examples to verify the theoretical findings and show the good performance of the proposed method. We delegate all proofs to the appendix.

1.1 Literature

Community detection in the offline setting (i.e., when the samples are collected beforehand and inference is made in one-shot) is a well-studied problem (see [13] for a survey). For example, spectral methods based on eigenvectors of the graph Laplacian are used in [14, 15]. Besides, there are many practical algorithms for community detection (see, e.g., [16]), including the so-called Kernighan–Lin algorithm [17] which uses a greedy algorithm to improve an initial division of the network and a genetic algorithm named Ga-net [18] to detect the community structure by calculating the community score. However, offline community detection cannot be used to detect community changes if the graph is dynamic.

Online community detection has also been considered in the literature. Peel and Clauset [10] first formalized the

change-point detection problem as identifying the times at which the large-scale patterns of interaction change fundamentally. They choose from a parametric family of probability distribution to describe the data and then use the Bayesian method to detect the change. A Markov-process-based approach is presented by [19] which is based on MCMC. Each graph snapshot depends on the current generative model and the previously observed snapshot. Moreover, [20] proposes a method called Spotlight to detect anomalies in streaming graphs by composing a K -dimensional sketch containing K subgraphs to detect changes inside the dynamic graph. Recently, a Laplacian anomaly detection method for dynamic graphs is presented in [21] which uses the spectrum of the Laplacian matrix of the graph structure at each snapshot to obtain low dimensional embeddings. However, none of these works gives a statistical perspective and asymptotic analysis for the quickest change detection in communities. While estimating the community structure through a dynamic network, our paper presents novel methods of handling estimation and change detection, which are supported by theoretical asymptotic optimality.

Spectral graph change detection is also related to our work. The spectral property of the graph is one of the essential theories that can capture the community structure of the graph. The spectral method proposed by [22] is used to detect changes in Noisy Dynamic Networks efficiently by transforming a graph to a lower-dimensional latent Euclidean space. In our work, we also use the spectral method to get a reduced dimensional representation for each node, and our procedure can detect different types of changes and has theoretically proved optimally.

Change Detection of Gaussian Graphical Model is similar to our work as well. We consider the Gaussian graphical model to capture the network structure through the inverse covariance matrix of the nodal features. The Gaussian model is useful for modeling the correlation between observations at different nodes. There are many previous works that are focused on the estimation of Gaussian graphical model. For instance, penalized likelihood method is proposed by [23] for estimating the concentration matrix in the Gaussian graphical model while [24] presents an alternative tuning-insensitive approach to efficiently choose the tuning parameter in finite sample settings. But none of these estimation of Gaussian graphical model can be directly used to detect the structure change. Recently, a piecewise stationary graphical models is presented in [25] and it is able to detect the change of graph by monitoring the conditional log-likelihood of all nodes in the network. However, this method does not consider the community structure of the network and thus is unable to distinguish different types of changes inside the network.

Manifold change detection is another type of area that is related to our work. In the work of [26], multi-scale online manifold learning is used to extract change-point detection test statistics from high-dimensional data. But they do not consider the network property for the high-dimensional data, thus cannot be applied directly to graph scenarios.

2 Problem Setup

Consider a dynamic network with n nodes. Assume at each time t , we observe a feature value v_{ti} for each node i , $i = 1, \dots, n$. We collect all features at each time into one vector and denote as $v_t \in \mathbb{R}^n, t = 1, 2, \dots$. We will focus on the online setting where we observe feature values sequentially. Such setting is widely applicable in real datasets, see below for some examples.

- In sensor networks, the feature $\{v_{ti}, t = 1, 2, \dots\}$ represent a sequence of signals recorded by the i -th sensor. The sensors may form communities and thus the features can be correlated. It can be the observed seismic/solar activity measurement from each sensor at each time in a seismic/solar system.
- In social networks, a vector of features represents user activities at each time. For instance, it can be social activities such as twittering at time t from each user in the Twitter network.

Assume the features for nodes within the same community have a higher correlation than those that are not in the same community. The correlation can be estimated using observed nodal features [27]. The underlying community structure may change at some time, which leads to a change in the correlations between the affected nodes and thus the distribution of feature vectors. We aim to detect such a change as quickly as possible from sequential observations.

In the following, we first give the community definition in Section 2.1 and statistical modeling for the community structure within graphs, then discuss two kinds of changes respectively in Section 2.2.

2.1 Adjacency matrix for community

Suppose there are m communities within a network with n nodes. Denote these communities as m sets $\{C_1, \dots, C_m\}$, where the k -th community is represented using the index set C_k of the nodes belonging to this community. Assume the communities do not overlap with each other, i.e., the index sets are mutually disjoint. For each node i , we introduce an indicator vector $a_i \in \{0, 1\}^m$ representing its true membership: the k -th entry equal to 1 and all other entries equal to 0 if node i belongs to the k -th community C_k , i.e.,

$$a_i = [0 \cdots \underbrace{1}_{k\text{-th entry}} \cdots 0]^\top, \forall i \in C_k.$$

Define the global indicator matrix as

$$A = [a_1, \dots, a_n]^\top \in \{0, 1\}^{n \times m}. \quad (1)$$

Notice that we have

$$a_i^\top a_j = \begin{cases} 1 & \text{if } \exists k \text{ s.t. nodes } i, j \in C_k, \\ 0 & \text{otherwise.} \end{cases}$$

Therefore, the matrix $AA^\top \in \{0, 1\}^{n \times n}$ defines an *adjacency matrix*, whose (i, j) -th entry equals to 1 if and only if nodes i and j belong to the same community. This setup for A can also be generalized beyond 0-1 matrices. For example, we may let $a_i \in \mathbb{R}^m$ represents a feature embedding vector for node i and each entry of a_i represents the weight/probability for node i belonging to the corresponding community.

2.2 Community change-point detection

We aim to monitor two types of structural changes in dynamic networks:

- i) The emergence of new communities: Before the change happens, there is no clear community formed in the graph, and the community structure emerges after the change, as indicated in Figure 1(a).
- ii) Switching membership: Some community members are switched after the change, such as the increase or decrease of a single community or the membership flow from one community to another, as indicated in Figure 1(b).

We now formulate such change detection problems based on the adjacency matrix representation in Section 2.1.

2.2.1 Emerging community

In many applications, the change can be modeled as the emergence of several disjoint communities; the nodes inside the same community are more correlated with each other. Thus, we start by considering the emerging community

detection problem, which assumes that the network has no community structure at the beginning but forms m communities (C_1, \dots, C_m) after the change where C_k is the node index set for the k -th community.

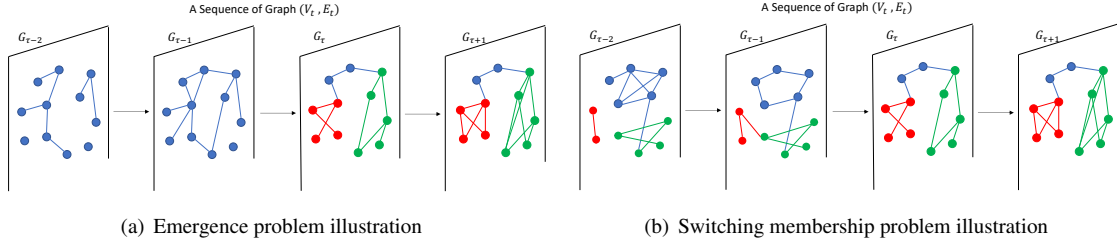


Figure 1: Case of emergence of communities after change time τ as shown in (a) and switching membership case shown in (b). Three communities are marked as red, blue, and green dots. For emergence problem, it can be seen that there is no community or one single community before changes happens, then after that three separate communities emerge. For switching membership case, it can be seen that before change happens, the blue community is the biggest one, while after the change, the membership of it begins switching to the other two communities.

With the indicator matrix A defined in (1), we assume the feature observations v_t is multivariate Gaussian and its covariance matrix is modeled based on the adjacency matrix AA^\top . More specifically, we cast the emerging community problem as follows.

$$\begin{aligned}
 H_0 : v_t &\stackrel{\text{i.i.d.}}{\sim} \mathcal{N}(0, \frac{1}{\sigma^2}I), \quad t = 1, 2, \dots \\
 H_1 : v_t &\stackrel{\text{i.i.d.}}{\sim} \mathcal{N}(0, \frac{1}{\sigma^2}I), \quad t = 1, 2, \dots, \tau, \\
 &v_t \stackrel{\text{i.i.d.}}{\sim} \mathcal{N}(0, (AA^\top + \sigma^2I)^{-1}), \quad t = \tau + 1, \tau + 2, \dots
 \end{aligned} \tag{2}$$

Here we introduce σ^2I as a noise term since the network is usually not perfectly separable in practice. We represent the Gaussian model using the inverse covariance matrix because this can be related to the Gaussian graphical model. Therefore, it is more meaningful to use the inverse covariance to represent the community structure. Following this, we can regard AA^\top as the underlying community structure of the graph and σ^2 as the noise level.

The above representation can be related to Gaussian graphical model, which is a common approach to exploring the relationships between nodes in a undirected graph through the inverse covariance matrix. Given a Gaussian graphical model with covariance matrix Σ , there is an edge between node i and node j , if and only if $\Sigma_{ij}^{-1} \neq 0$. Note that this can be related to our model: the zero-valued entry in the inverse covariance matrix means that the corresponding edge does not exist in the graphical model. As the inverse covariance matrix changes from σ^2I to $AA^\top + \sigma^2I$ in model (2), the corresponding off-diagonal entries change from zero to non-zero after the community emerges.

2.2.2 Switching membership

Another type of community change is called the switching membership problem. As shown in Figure 1(b), some of the nodes belong to one community at first and switch to a different one after the change happens at time τ . Similar to (2), the switching membership problem can be formulated as follows:

$$\begin{aligned}
 H_0 : v_t &\stackrel{\text{i.i.d.}}{\sim} \mathcal{N}(0, (A_1A_1^\top + \sigma^2I)^{-1}), \quad t = 1, 2, \dots \\
 H_1 : v_t &\stackrel{\text{i.i.d.}}{\sim} \mathcal{N}(0, (A_1A_1^\top + \sigma^2I)^{-1}), \quad t = 1, 2, \dots, \tau, \\
 &v_t \stackrel{\text{i.i.d.}}{\sim} \mathcal{N}(0, (A_2A_2^\top + \sigma^2I)^{-1}), \quad t = \tau + 1, \tau + 2, \dots
 \end{aligned} \tag{3}$$

Here A_1 represents the pre-change community structure while A_2 represents the post-change community structure. This general model can denote cases when the sizes of certain communities change. It can also model the case when the total number of communities increases (one community splits into smaller ones) or decreases (several small communities merge into a bigger one). As a result, the emergence problem can be seen as a special case of the switching membership problem, which is capable of detecting various types of graph structure changes. We will show later the detecting procedure of switching membership can also be equivalently treated as an emergence problem.

3 Detection Procedures

In this section, we first review the well-known cumulative sum (CUSUM) detection rule and then propose the Spectral-CUSUM procedure under both emergence and switching membership scenarios.

3.1 Exact-CUSUM procedure

Let $f_\infty(\cdot)$ and $f_0(\cdot)$ denotes the pre- and post-change probability density function (pdf) of the observations, and \mathbb{E}_∞ and \mathbb{E}_0 denotes the expectation under f_∞ and f_0 , respectively. The CUSUM statistic [28] is defined by maximizing the log-likelihood ratio statistic over all possible change-point locations:

$$S_t = \max_{1 \leq k \leq t} \sum_{i=k}^t \log \frac{f_0(v_i)}{f_\infty(v_i)}.$$

S_t has a recursive formulation with $S_0 = 0$ as follows:

$$S_t = (S_{t-1})^+ + \log \frac{f_0(v_t)}{f_\infty(v_t)}, \quad t \geq 1,$$

where $(x)^+ := \max\{x, 0\}$. The corresponding CUSUM stopping time T_C is defined as:

$$T_C = \inf\{t > 0 : S_t \geq b\}, \quad (4)$$

where b is a pre-set constant threshold. Under the model (2), we have that

$$\log \frac{f_0(v_t)}{f_\infty(v_t)} = -\frac{1}{2} v_t^\top A A^\top v_t + \frac{1}{2} \log \frac{\det(AA^\top + \sigma^2 I)}{\sigma^{2n}}.$$

Since the multiplicative factor $1/2$ is positive, we can omit it from the log-likelihood ratio when forming the CUSUM statistic, thus yielding an equivalent formulation:

$$S_t = (S_{t-1})^+ - \underbrace{v_t^\top A A^\top v_t}_{d} + \log \frac{\det(AA^\top + \sigma^2 I)}{\sigma^{2n}}, \quad (5)$$

where d is a drift parameter which is fixed in the CUSUM procedure.

Similarly, for the switching membership problem under the model (3), the log-likelihood ratio is:

$$\begin{aligned} \log \frac{f_0(v_t)}{f_\infty(v_t)} &= -\frac{1}{2} v_t^\top (A_2 A_2^\top - A_1 A_1^\top) v_t \\ &\quad + \frac{1}{2} \log \frac{\det(A_2 A_2^\top + \sigma^2 I)}{\det(A_1 A_1^\top + \sigma^2 I)}. \end{aligned}$$

Therefore, the CUSUM statistic in this case becomes:

$$S_t = (S_{t-1})^+ - v_t^\top (A_2 A_2^\top - A_1 A_1^\top) v_t + \underbrace{\log \frac{\det(A_2 A_2^\top + \sigma^2 I)}{\det(A_1 A_1^\top + \sigma^2 I)}}_{d'}. \quad (6)$$

We note that in the exact CUSUM procedure, all the parameters are assumed known so that the drift terms d and d' can be computed exactly beforehand.

3.2 Spectral-CUSUM procedure

The implementation of the exact CUSUM procedure requires that all parameters are known, and it has been proved to be optimum [29, 30]. However, if the post-change distribution is unknown, the exact-CUSUM is not applicable. Usually, we can estimate the pre-change distribution using historical data (training data), but the post-change community structures are unknown since it represents anomaly information and cannot be predicted. Therefore, the post-change distribution, i.e., the post-change structure A , has to be estimated sequentially from data. A natural estimate for the post-change covariance matrix $(AA^\top + \sigma^2 I)^{-1}$ is the sample covariance matrix. To eliminate the matrix inversion computation in estimating A , we use eigendecomposition on the sample covariance matrix to estimate A directly. Therefore, we propose the Spectral-CUSUM procedure below where we approximate the covariance matrix by rank- m eigendecomposition.

Define $U \in \mathbb{R}^{n \times m}$ and $\Lambda \in \mathbb{R}^{m \times m}$ as the eigenvectors and eigenvalues of the term AA^\top within the post-change covariance matrix, i.e., $AA^\top = U\Lambda U^\top$. Here Λ is a diagonal matrix corresponding to the eigenvalues of the matrix AA^\top defined using (1):

$$\Lambda = \begin{bmatrix} |C_1| & & \\ & \ddots & \\ & & |C_m| \end{bmatrix},$$

where $|C_k|$ denotes the number of nodes inside the k -th community, here without loss of generality we assume $|C_1| > |C_2| > \dots > |C_m|$. This shows that the eigenvalue decomposition of the adjacency matrix would reflect the community structure of a graph, which can also provide empirical guidance on how to determine the potential number m of communities.

We can then jointly estimate matrices U and Λ . Using observations $\{v_{t+1}, \dots, v_{t+w}\}$ in a *future* sliding window with length w , we define

$$\hat{G}_t = (v_{t+1} v_{t+1}^\top + \dots + v_{t+w} v_{t+w}^\top) / w. \quad (7)$$

Note that \hat{G}_t serves as an approximation for the covariance matrix $(AA^\top + \sigma^2 I)^{-1}$ if samples $\{v_{t+1}, \dots, v_{t+w}\}$ are drawn from post-change distribution. Let $\{\hat{u}_{t1}, \dots, \hat{u}_{tm}\}$ be the m unit-norm eigenvectors corresponding to the m *smallest* eigenvalues $\{\hat{\lambda}_{t1}, \dots, \hat{\lambda}_{tm}\}$ of \hat{G}_t . Let

$$\hat{U}_t = [\hat{u}_{t1}, \dots, \hat{u}_{tm}] \in \mathbb{R}^{n \times m},$$

and

$$\hat{\Lambda}_t = \text{diag}(\hat{\lambda}_{t1}, \dots, \hat{\lambda}_{tm}) \in \mathbb{R}^{m \times m}.$$

Then A can be approximately estimated using $\hat{A}_t = \hat{U}_t \hat{\Lambda}_t^{-1/2}$, as the noise term σ^2 is usually relatively small. Then we can substitute the estimate \hat{A}_t into (5) to obtain an alternative detection statistics, which we call Spectral-CUSUM, when the post-change distribution is unknown:

$$\mathcal{S}_t = (\mathcal{S}_{t-1})^+ - v_t^\top \hat{A}_t \hat{A}_t^\top v_t + d. \quad (8)$$

Here d is a tunable drift parameter that plays a similar role as the last term in (5). And the stopping time is defined as:

$$\mathcal{T}_C = \inf\{t > 0 : \mathcal{S}_t \geq b\}. \quad (9)$$

Similarly, for the switching membership problem, the alternative to (6) is:

$$\mathcal{S}_t = (\mathcal{S}_{t-1})^+ - v_t^\top (\hat{A}_t \hat{A}_t^\top - A_1 A_1^\top) v_t + d'. \quad (10)$$

In the proposed Spectral-CUSUM procedure, the drift parameter d should be chosen to ensure the detection statistics is capable of detecting the change. More specifically, the CUSUM type procedure requires the increment term in \mathcal{S}_t to have a *negative* mean under the pre-change distribution and a *positive* mean under the post-change distribution. Therefore, for the emerging community problem we need:

$$\mathbb{E}_0[v_t^\top \hat{A}_t \hat{A}_t^\top v_t] < d < \mathbb{E}_\infty[v_t^\top \hat{A}_t \hat{A}_t^\top v_t]. \quad (11)$$

For the switching membership problem, the same rule means that we need:

$$\mathbb{E}_0[v_t^\top (\hat{A}_t \hat{A}_t^\top - A_1 A_1^\top) v_t] < d' < \mathbb{E}_\infty[v_t^\top (\hat{A}_t \hat{A}_t^\top - A_1 A_1^\top) v_t]. \quad (12)$$

Since A_1 is a constant matrix known beforehand from history data, we can calculate the expectations $\mathbb{E}[v_t^\top A_1 A_1^\top v_t]$ explicitly. Thus, the switching membership problem can be treated as an emerging community problem. Therefore, the theoretical analysis for the switching membership problem is similar to the emerging community problem, and we will only discuss the emergence problem in Section 4.

Due to the above property (11) which is also mentioned in [31, 32], the detection statistic in (8) will deviate from 0 and increase gradually after the change happens.

Algorithm 1 Spectral-CUSUM procedure

Input: Sequence of observations $\{v_t, t = 1, 2, \dots\}$, number of communities m , sliding window size w , carefully selected drift parameter d (or d'), detection threshold b .

Output: Stopping time \mathcal{T}_C .

- 1: Initialize $\mathcal{T}_C = \infty, t = 0, S_0 = 0$.
 - 2: **while** $S_t < b$ **do**
 - 3: Calculate sample covariance matrix \hat{G}_t from future observations using (7);
 - 4: Compute \hat{U}_t and $\hat{\Lambda}_t$ through the eigenvalue decomposition of \hat{G}_t ;
 - 5: Estimate community structure $\hat{A}_t = \hat{U}_t \hat{\Lambda}_t^{-1/2}$;
 - 6: Let $t = t + 1$ and update Spectral-CUSUM statistics S_t following (8) or (10).
 - 7: **Set** $\mathcal{T}_C = t$.
 - 8: **return** \mathcal{T}_C
-

4 Theoretical Analysis

This section provides theoretical analysis of the proposed Spectral-CUSUM procedure under the emerging community setting. The main result is presented in Theorem 2, which shows the asymptotic optimality of Spectral-CUSUM under the optimal choices of parameters. We also derive the form of the optimal parameters. The analysis techniques are related and extension to those used in prior works in [33] and in [34, 35] for subspace change detection.

4.1 Preliminary

We first state the following assumptions that are being made in order to derive the main results.

Assumption 4.1. *We make the following assumptions for the true community structure.*

1. *The total number of communities remains a constant value m during the detection procedure.*
2. *The noise term σ^2 on covariance matrix is relatively small in the order of $\sigma^2 = o(1)$.*

We note that Assumption 4.1 (1) enables us to pre-define the value of m before performing the rank- m eigenvalue decomposition on the sample covariance matrix; Assumption 4.1 (2) is reasonable since the white noise is less significant when the length of observations is long enough.

We first introduce the following notations to simplify the presentation of main results:

$$B_i = \sum_{k=1, k \neq i}^m \frac{\lambda_i \lambda_k}{(\lambda_i - \lambda_k)^2}, \quad D = \sum_{i=1}^m \left(1 - \frac{B_i}{w} + \frac{3B_i^2}{w^2} \right),$$

where λ_i is the i -th largest eigenvalue of the matrix AA^\top , and thus is approximately the inverse of the i -th smallest eigenvalue of the covariance matrix $(AA^\top + \sigma^2 I)^{-1}$ under Assumption 4.1 (2), w is the sliding window size, and σ^2 is the noise level.

We start with a useful result in [36].

Theorem 1 (Asymptotic Property of Sample Covariance, [36]). *The asymptotic distribution of eigenvectors and eigenvalues of sample covariance matrix under post-change regime of model (2) are (i) independent and (ii) has the follow-*

ing distribution under the assumption that the eigenvalues are distinct:

$$\sqrt{w}(\hat{u}_i - u_i) \xrightarrow{d} \mathcal{N}\left(0, \sum_{k=1, k \neq i}^n \frac{\lambda_i \lambda_k}{(\lambda_i - \lambda_k)^2} u_k u_k^\top\right),$$

$$\sqrt{w}(\hat{\lambda}_i - \lambda_i) \xrightarrow{d} \mathcal{N}(0, 2\lambda_i^2),$$

where \xrightarrow{d} denotes convergence in distribution. Here \hat{u}_i and $\hat{\lambda}_i$ denotes the sample eigenvectors and eigenvalues, while u_i and λ_i denotes the eigenvectors and eigenvalues of the true covariance matrix, and n is the data dimension.

For the emerging community problem model in (2), the post-change covariance matrix is $(AA^\top + \sigma^2 I)^{-1}$. Recall that we use the window size w to construct the post-change sample covariance matrix in (7) and then estimate the eigenvalues and eigenvectors. Denote $\rho_1 < \dots < \rho_m$ as the smallest m eigenvalues of $(AA^\top + \sigma^2 I)^{-1}$, i.e., $\rho_i = 1/(\sigma^2 + |C_i|)$, and let $\{u_i, i = 1, \dots, m\}$ denotes the corresponding eigenvectors. Let $\hat{\rho}_i$ and $\hat{u}_i, i = 1, \dots, m$, be the smallest m eigenvalues and corresponding eigenvectors obtained from the sample covariance matrix \hat{G}_t . Then by Theorem 1, we have

$$\sqrt{w}(\hat{\rho}_i - \rho_i) \xrightarrow{d} \mathcal{N}(0, 2\rho_i^2),$$

and

$$\sqrt{w}(\hat{u}_i - u_i) \xrightarrow{d} \mathcal{N}\left(0, \sum_{k=1, k \neq i}^m \frac{\rho_i \rho_k}{(\rho_i - \rho_k)^2} u_k u_k^\top + \frac{\rho_i / \sigma^2}{(\rho_i - 1/\sigma^2)^2} (I - UU^\top)\right),$$

note that the second term in the above covariance matrix

$$\frac{\rho_i / \sigma^2}{(\rho_i - 1/\sigma^2)^2} (I - UU^\top) = \frac{\sigma^2(\sigma^2 + |C_i|)}{|C_i|^2} (I - UU^\top)$$

is small when σ^2 is small. Thus, under the Assumption 4.1 (2), we can make the approximation by omitting the second term when we have repeated eigenvalues.

Then, with the help of Theorem 1 we can show the following properties for Spectral-CUSUM.

Lemma 1 (Properties of detection statistic for Spectral-CUSUM). *The expected drifts under the pre- and post-change distributions for Spectral-CUSUM are given by*

$$\mathbb{E}_\infty[v_t^\top \hat{A}_t \hat{A}_t^\top v_t] = m,$$

$$\mathbb{E}_0[v_t^\top \hat{A}_t \hat{A}_t^\top v_t] = \sum_{i=1}^m \left(1 - \frac{B_i}{w} + \frac{3B_i^2}{w^2}\right).$$

The proof of this Lemma is shown in the Appendix.

4.2 ARL/EDD performance analysis

The most common performance of change detection procedures is measured by average run length (ARL) and expected detection delay (EDD). ARL represents the average time interval between two consecutive false alarms, while EDD measures the worst-case detection delay. When ARL is fixed, it is known that the exact CUSUM procedure minimizes

EDD, which can be calculated directly. In the following, we will compute ARL and EDD for the proposed Spectral-CUSUM procedure given in (8) for the emerging community problem.

Given a constant $\gamma > 1$ as the desired lower bound of ARL, we need to set the threshold b in (4) (and similarly in (9) for Spectral-CUSUM) accordingly such that $\text{ARL} \geq \gamma$. Recall that T_C denotes the stopping time for the exact CUSUM procedure. Thus $\mathbb{E}_0[T_C]$ and $\mathbb{E}_\infty[T_C]$ are EDD and ARL of CUSUM. Similarly, $\mathbb{E}_0[\mathcal{T}_C]$ and $\mathbb{E}_\infty[\mathcal{T}_C]$ are the EDD and ARL of Spectral-CUSUM. According to classic results from [37], we have the following:

$$\mathbb{E}_\infty[T_C] = \frac{e^b}{\mathcal{I}_\infty}(1 + o(1)), \quad \mathbb{E}_0[T_C] = \frac{b}{\mathcal{I}_0}(1 + o(1)), \quad (13)$$

where \mathcal{I}_0 and \mathcal{I}_∞ are the Kullback-Leibler (KL) information number:

$$\mathcal{I}_0 = \mathbb{E}_0\{\log[f_0(x)/f_\infty(x)]\},$$

$$\mathcal{I}_\infty = \mathbb{E}_\infty\{\log[f_\infty(x)/f_0(x)]\}.$$

The constraint $\text{ARL} \geq \gamma$ will be satisfied with threshold $b = (\log \gamma)(1 + o(1))$ according to (13). Substitute the threshold into the EDD formulation, we obtain the relationship between EDD and ARL (γ) as

$$\begin{aligned} \mathbb{E}_0[T_C] &= \frac{\log \gamma}{\mathcal{I}_0}(1 + o(1)) \\ &= \frac{2 \log \gamma}{\log \frac{\det(AA^\top + \sigma^2 I)}{\sigma^{2n}} - \sum_{i=1}^m \frac{\lambda_i}{\sigma^2 + \lambda_i}}(1 + o(1)), \end{aligned}$$

where λ_i is the i -th largest eigenvalue of the matrix AA^\top .

For performance analysis of Spectral-CUSUM, we follow a similar strategy as [34], where the analysis is done for a different problem, subspace detection, for a special rank-one case; here, to generalize the analysis, we extend it for higher rank cases. since the increment $-v_t^\top \hat{U}_t \hat{\Lambda}_t^{-1} \hat{U}_t^\top v_t + d$ in (8) is not exactly a log-likelihood ratio, we need to introduce an equalizer δ_∞ such that:

$$\mathbb{E}_\infty[\exp\{\delta_\infty[-v_t^\top \hat{U}_t \hat{\Lambda}_t^{-1} \hat{U}_t^\top v_t + d]\}] = 1. \quad (14)$$

Note that when (14) holds, $\delta_\infty[-v_t^\top \hat{U}_t \hat{\Lambda}_t^{-1} \hat{U}_t^\top v_t + d]$ is the log-likelihood ratio between \tilde{f}_0 and f_∞ where

$$\tilde{f}_0 = \exp\{\delta_\infty[-v_t^\top \hat{U}_t \hat{\Lambda}_t^{-1} \hat{U}_t^\top v_t + d]\} f_\infty.$$

This allows us to compute the threshold b asymptotically.

Similar to the derivation in [34], we have that:

$$\mathbb{E}_0(\mathcal{T}_C) = \frac{\log \gamma(1 + o(1))}{\delta_\infty(\mathbb{E}_0[-v_t^\top \hat{U}_t \hat{\Lambda}_t^{-1} \hat{U}_t^\top v_t] + d)} + w,$$

where the window length w is added for the reason that we are using future data to detect the potential change at time t , thus the actual detection time is $t + w$. Using standard computations involving Moment Generating Function for

Gaussian random variables we can write:

$$\begin{aligned}
& \mathbb{E}_\infty [e^{\delta_\infty [-v_t^\top \hat{A}_t \hat{A}_t^\top v_t + d]}] \\
&= e^{\delta_\infty d} \mathbb{E} \left[\mathbb{E}_\infty [e^{-\delta_\infty [v_t^\top \hat{A}_t \hat{A}_t^\top v_t]} | \hat{A}_t] \right] \\
&= e^{\delta_\infty d} \mathbb{E} \left[\int e^{-\delta_\infty (v_t^\top \hat{A}_t \hat{A}_t^\top v_t)} \frac{e^{-v_t^\top v_t \sigma^2 / 2}}{\sqrt{(2\pi)^n (1/\sigma^2)^n}} dv_t \right] \\
&= e^{\delta_\infty d} \mathbb{E}_\infty \left[|I + 2\sigma^{-2} \delta_\infty \hat{A}_t \hat{A}_t^\top|^{-1/2} \right] \\
&= \frac{e^{\delta_\infty d}}{\sqrt{\prod_{i=1}^m (1 + 2\sigma^{-2} \delta_\infty / \rho_i)}} = 1.
\end{aligned} \tag{15}$$

We use the standard technique of ‘‘completing the square’’ in the exponent. With proper normalization, we generate an alternative Gaussian pdf which integrates to 1. Solving (15) we get:

$$d = \frac{\sum_{i=1}^m \log(1 + 2\sigma^{-2} \delta_\infty / \rho_i)}{2\delta_\infty}.$$

We notice that under the pre-change measure all eigenvalues ρ_i of the covariance matrix equal to $1/\sigma^2$, thus the drift parameter can be further written as:

$$d = \frac{m \log(1 + 2\delta_\infty)}{2\delta_\infty}. \tag{16}$$

Combining Lemma 1 and Equation (16) we have expression for EDD as:

$$\begin{aligned}
& \mathbb{E}_0(\mathcal{T}_C) \\
&= \frac{2 \log \gamma(1 + o(1))}{-2\delta_\infty \sum_{i=1}^m (1 - \frac{B_i}{w} + \frac{3B_i^2}{w^2}) + m \log(1 + 2\delta_\infty)} + w.
\end{aligned} \tag{17}$$

4.3 Asymptotic optimality of Spectral-CUSUM

Note that the formulation (17) contains two parameters: the drift d (or δ_∞) and the window size w . We can further optimize over these two parameters to obtain the minimal EDD, then prove that the Spectral-CUSUM procedure based on optimal window size and draft is first-order asymptotically optimum.

We now derive the optimal design of two parameters: window size w and drift parameter d . The theoretical analysis is of great importance because it serves as a guideline for choosing the best parameters used in the proposed community detection procedure. Usually, Monte Carlo simulation is used to determine the threshold. However, Monte Carlo simulation can be very time-consuming, especially for large networks such as Twitter social networks. In such cases, the threshold obtained from the theoretical analysis can be a good approximation and significantly reduce computational costs. Figure 3 shows numerical examples of choosing the optimal window size w .

We first find the optimal value of δ_∞ and thus the drift d (according to (16)). We observe that the denominator in (17) is a concave function of δ_∞ therefore, it exhibits a single maximum. Setting the derivative of the denominator as a function of δ_∞ to be 0, we obtain the optimum value of δ_∞ (we omit the high order terms of eigenvalue in the product):

$$\delta_\infty^* = \frac{m}{2 \sum_{i=1}^m (1 - B_i/w + 3B_i^2/w^2)} - \frac{1}{2} = \frac{m}{2D} - \frac{1}{2}. \tag{18}$$

Substituting δ_∞^* to (17), we have:

$$\mathbb{E}_0(\mathcal{T}_C) = \frac{2 \log \gamma (1 + o(1))}{D - m + m \log(m/D)} + w. \quad (19)$$

Thus the remaining step is to find the optimal window size w^* such that (19) is minimized. After taking derivative with respect to w , note that $1/w^2$ is in the order of $o(1/w)$ thus can be ignored when w is large. Thus we omit all the higher-order terms of w in D . The final results are summarized in Lemma 2.

Lemma 2 (Optimal window size and drift parameter). *For each ARL level γ , the optimal window size w^* which minimizes the Expected Detection Delay (EDD) is given by:*

$$w^* = \frac{\sqrt{2 \log \gamma \left(\frac{1}{1 - \delta D/m} - 1 \right) \left(\sum_{i=1}^m \frac{\lambda_i B_i}{\sigma^2 + \lambda_i} \right)}}{-m + \sum_{i=1}^m \frac{\lambda_i}{\sigma^2 + \lambda_i} - m \log \left(\sum_{i=1}^m \frac{\lambda_i}{m \sigma^2 + m \lambda_i} \right)}. \quad (20)$$

Putting optimal w^* and δ_∞^* back into (16) gives the optimal value for drift parameter:

$$d^* = \frac{m \log(m/D^*)}{m/D^* - 1}, \quad (21)$$

where

$$D^* = \sum_{i=1}^m (1 - B_i/w^* + 3B_i^2/w^{*2}).$$

The proof of this Lemma is shown in the Appendix.

Then by applying the optimal window size of w^* and calculating the ratio, we can show the corresponding Spectral-CUSUM is first-order asymptotically optimum with respect to the exact CUSUM, which has the smallest EDD as shown in [29] and [30]. The following is our main theorem.

Theorem 2 (Optimality of Spectral-CUSUM). *Assuming ARL is the same, the ratio between the EDD of the Spectral-CUSUM and the EDD of the exact CUSUM satisfies:*

$$\frac{\mathbb{E}_0[\mathcal{T}_C]}{\mathbb{E}_0[T_C]} = 1 + (\log \gamma)^{-\frac{1}{2}} \cdot \tilde{C} + o(1). \quad (22)$$

where

$$\tilde{C} = \frac{\sqrt{\left(\frac{2}{1 - \delta D/m} - 2 \right) \sum_{i=1}^m \frac{\lambda_i B_i}{\sigma^2 + \lambda_i} \left(\log \frac{\det(AA^\top + \sigma^2 I)}{\sigma^{2n}} - \sum_{i=1}^m \frac{\lambda_i}{\sigma^2 + \lambda_i} \right)}}{2[-m + \sum_{i=1}^m \frac{\lambda_i}{\sigma^2 + \lambda_i} - m \log \left(\sum_{i=1}^m \frac{\lambda_i}{m \sigma^2 + m \lambda_i} \right)]}.$$

When $\gamma \rightarrow \infty$, for fixed m, n, σ bounded away from zero, this ratio $\mathbb{E}_0[\mathcal{T}_C]/\mathbb{E}_0[T_C]$ tends to 1, i.e., the Spectral-CUSUM is asymptotically optimum.

5 Efficient Computation by Subspace Tracking

In this section, we present an efficient algorithm to keep track of the underlying community structure even if we do not assume the form of the graph structure. This can be treated as a complementary approach to the proposed Spectral-CUSUM method when we have low confidence or lack of pre-change observations. Inspired by the GROUSE algorithm [38] which implements stochastic gradient descent on the Grassmann manifold to update subspaces at each

time slot, we design a subspace tracking algorithm to update the estimated subspace, denoted as \hat{Q}_t , each time a new graph observation G_t arrives. Here we consider graph observation instead of vector observation v_t on nodes. Similar to (7), the graph observation at time t can be represented using vector observation as $G_t = v_t v_t^\top$.

If we treat each observation as a static graph and apply the spectral clustering method in [39] at each time, we would get a sequence of \hat{Q}_t independently, which is quite time-consuming and not guaranteed to converge if considering noisy cases. Instead, we can perform an updating procedure each time on $Q \in \mathbb{R}^{n \times m}$ on a Grassmann manifold. The Grassmannian denoted as $\text{Gr}(m, n)$ is a space that contains all m -dimensional linear subspaces of the n -dimensional vector space. As a compact Grassmann manifold, its geodesics can be computed as indicated in [40]. Our target matrix Q can then be represented as a point in the Grassmann manifold. Thus the optimization problem becomes finding optimized \hat{Q} such that:

$$\hat{Q} = \arg \min_{Q \in \mathbb{R}^{n \times m}} \sum_t \text{tr}(Q^\top G_t Q), \text{ s.t. } Q^\top Q = I.$$

We consider the problem for every time slot and define function $f_t(Q) = \text{tr}(Q^\top G_t Q)$ and the derivative of f_t with respect to Q is [41]:

$$\frac{df_t}{dQ} = \frac{d(\text{tr}(Q^\top G_t Q))}{dQ} = (G_t + G_t^\top)Q. \quad (23)$$

Then we use Equation (2.70) in [40] to get the gradient of function $f_t(Q)$ on Grassmann manifold from (23):

$$\nabla f_t = (I - QQ^\top) \frac{df_t}{dQ} = (I - QQ^\top)(G_t + G_t^\top)Q.$$

Gradient descent algorithm along a Grassmann manifold is given by equation (2.65) in [40], proving that it is a function of the singular values and vectors of ∇f_t , so suppose we have got the reduced Singular Value Decomposition (rSVD) of $-\nabla f_t = U\Sigma V^\top$ where only the top- k eigenvalues and eigenvectors are kept so that the computational cost is much reduced, we can write the updating function with a step size η as:

$$Q(\eta) = \begin{pmatrix} QV & U \end{pmatrix} \begin{pmatrix} \cos \Sigma\eta \\ \sin \Sigma\eta \end{pmatrix} V^\top. \quad (24)$$

Here we update Q with a step size η to get closer to the local minimum on the Grassmann manifold. The complete algorithm is shown in Algorithm 2.

Algorithm 2 Subspace Tracking for Spectral-CUSUM

Input: Weighted adjacency matrix at time t denoted as G_t , the total number of iterations T , number of communities m , a set of step sizes η_t .

Output: Subspace Representation Q of the graph.

- 1: Initialize Q randomly, introduce y as a T -dimensional vector with all entries equal to 0.
 - 2: **for** $t = 1, \dots, T$ **do**
 - 3: Observe current adjacency matrix G_t .
 - 4: Compute $\nabla f_t = (I - QQ^\top)(G_t + G_t^\top)Q$.
 - 5: Compute SVD of $-\nabla f_t = U\Sigma V^\top$.
 - 6: Update Q using (24) with step size η_t .
 - 7: Update $y(t) = \text{tr}(Q^\top G_t Q)$
 - 8: Run CUSUM detection procedure on y and get detection statistic S .
 - 9: **return** S
-

Choice of Step Size. For our problem, constant step size and decreasing step size can be efficient. The constant step is slower initially, but it is more stable to detect changes in community structures. In our numerical experiments, we take constant step size $\eta = 0.01$.

Complexity. In practice, we notice that in this algorithm, we have to perform SVD for each iteration, which is quite time-consuming. To accelerate the whole algorithm, we use the incremental SVD algorithm [42] in each iteration.

In practice, we have to perform SVD for each iteration in this algorithm, which is time-consuming. To accelerate the whole algorithm, we use an incremental SVD algorithm [42] in each iteration.

6 Numerical Experiments

In this section, we compare our method with the state-of-the-art and discuss their numerical results on both synthetic and real data sets. Since a graph can be considered as a discrete approximation to a manifold [43], we also show that our model can achieve promising performance on dynamic manifold data.

6.1 Methods for comparison

In our experiments, we compare our method with four other baseline approaches, including (1) Generalized Likelihood Ratio procedure based on vectorized data (Vectorized GLR) (2) Hotelling's T -squared CUSUM (Hotelling); (3) Single eigenvector procedure (SC, $m = 1$); (4) Rank- m Subspace Tracking of Section 5 (SGD); and (5) Exact CUSUM as a sanity check. The detailed explanation of these baseline methods are as follows:

(1) *Generalized Likelihood Ratio (GLR) procedure based on vectorized data.* This baseline method completely ignores the topology properties of the adjacency graph G_t and vectorizes it as $g_t = \text{vec}(G_t)$ such that the previous hypothesis test (2) becomes:

$$\begin{aligned} H_0 : g_t &\stackrel{\text{iid}}{\sim} \mathcal{N}(0, \sigma^2 I_{n^2}) & t = 1, 2, \dots, \tau \\ H_1 : g_t &\stackrel{\text{iid}}{\sim} \mathcal{N}(h, \sigma^2 I_{n^2}) & t = \tau + 1, \tau + 2, \dots \end{aligned} \quad (25)$$

where $h = \text{vec}(AA^\top)$. Then classical result from [29, 44] gives the optimal stopping criteria for GLR procedure:

$$T_{\text{GLR}} = \inf \left\{ t : \max_{t-w < k < t} \frac{(\sum_{i=k+1}^t \|g_i\|)^2}{t-k} > b \right\}. \quad (26)$$

(2) *Hotelling's T-squared CUSUM*. We also compare our method with Hotelling's T -squared statistic, which was introduced in [45]. The way to implement this is to calculate a pre-change sample mean $\hat{\mu}_0$ and sample covariance $\widehat{\Sigma}_0$, then keep track of the current sample mean $\bar{\mu}_{t-w,t}$ via a sliding window. We also need to pre-define the drift parameter d^{H_2} , which can be obtained from historical data. Thus the detection statistic is given by:

$$S_t^{H_2} = (S_{t-1}^{H_2})^+ + (\bar{\mu}_{t-w,t} - \hat{\mu}_0)^\top \widehat{\Sigma}_0^{-1} (\bar{\mu}_{t-w,t} - \hat{\mu}_0) - d^{H_2}.$$

Then the optimal stopping time for Hotelling's statistics is given by:

$$T^{H_2} = \inf \left\{ t > 0 : S_t^{H_2} \geq b \right\}. \quad (27)$$

(3) *Single eigenvector procedure of Spectral-CUSUM*. This baseline method is almost the same as proposed Spectral-CUSUM with the only difference of fixing community size $m = 1$. We use it to illustrate the importance of finding the optimal community size.

(4) *Rank- m Subspace Tracking*. This is proposed in Section 5 as a numerical alternative method for our Spectral CUSUM. So we list it as an another baseline.

For synthetic data, we study the relationship between ARL and EDD. For real data, we study EDD only since we cannot implement simulation to decide the average run length if the history data under pre-change distribution is not sufficient.

6.2 Synthetic experiments

We devise three synthetic experiments to study the performance of our method on the emergence and the switching membership problems.

Synthetic data 1 is used for evaluating our method on detecting emerging community. In this experiment, we set $\sigma = 5$ and assume a dynamic graph that contains 50 nodes without any community structure in the beginning. When the change occurs at time $t =$, three communities are formed, containing 10, 10, and 15 nodes, respectively. In other words, we have $m = 0$ before t and $m^* = 3$ after t . The optimal window size can be found according to (20), where $w = 5$.

The experimental result shows that our method significantly outperforms other baselines. Figure 2 presents the ARL of all the methods on the synthetic data 1 with different choices of community density and window size. As can be observed, our method (blue line) works much better (the lower, the better) than the baselines and is closest to the sanity check method Exact-CUSUM. A comparison of how community size would affect the choice of optimal window size is also shown in the figure 3(b) where we increase the size of each emerging community by 5, referred to as larger emerging communities. It can be inferred that the change becomes easier to detect in larger communities. Thus, the optimal window size decreases correspondingly. In figure 4, we show how different noise levels could infect the general detection delay, which leads to the conclusion that a larger noise level leads to a longer average detection delay. Moreover, when ARL is relatively small, a large noise level would not have much effect on the EDD. However, if the ARL is larger, the EDD will be increased significantly for higher noise levels.

Synthetic data 2 is used for evaluating our method on detecting switching membership. For the design of the switching membership experiment, the number of nodes is 50, and the size of the three communities remains the same: 10, 10, and 15 nodes. However, the membership for all three communities will change. A comparison between SGD, Exact-CUSUM, and Spectral-CUSUM is shown in Figure 5. We can see that the single eigenvector procedure

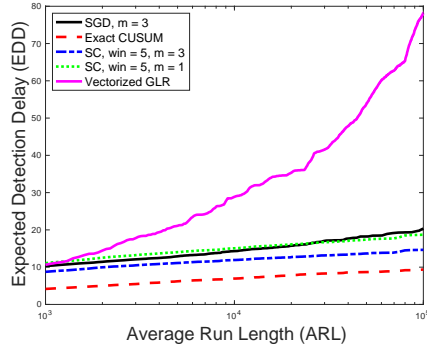


Figure 2: Comparison of the single eigenvector procedure and Exact-CUSUM procedure for emergence problem. Community size fixed and σ is set to be 5.

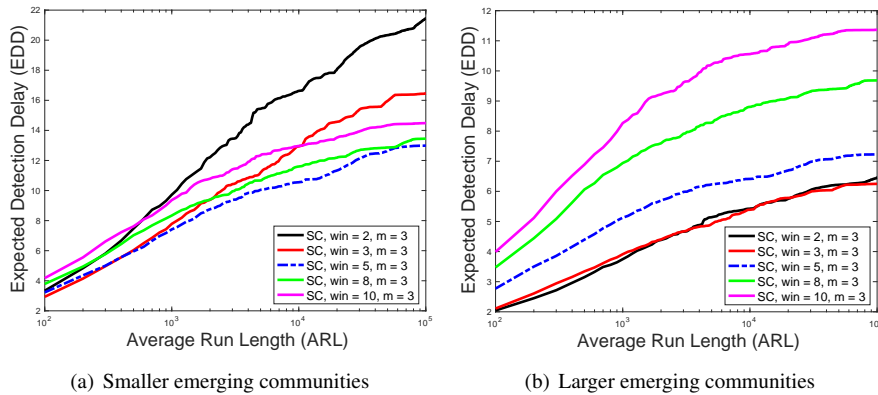


Figure 3: ARL vs EDD plot for Optimal window size for Spectral-CUSUM with smaller (a) and larger (b) emerging communities.

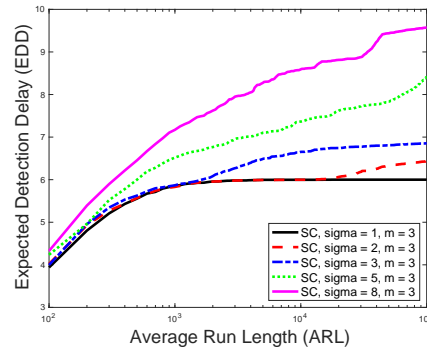


Figure 4: Comparison of the different noise level for emergence problem. Community size fixed and values of σ is set to be 1,2,3,5,8, respectively.

($m = 1$) performs much worse than Spectral-CUSUM using the correct potential community size ($m = 3$). The performance gain of spectral-CUSUM in the switching membership setup is larger than that in the emerging subspace problems compared with the Exact-CUSUM procedure. Moreover, the EDD of SGD is growing quite fast with the

increase of ARL, which indicates that it is noise-sensitive.

Here we do not compare with the vectorized GLR procedure since it does not work in the switching membership problem. The reason is that the switching membership change does not lead to the increase or decrease of average edge weights; thus, the change cannot be detected without considering the graph topology.

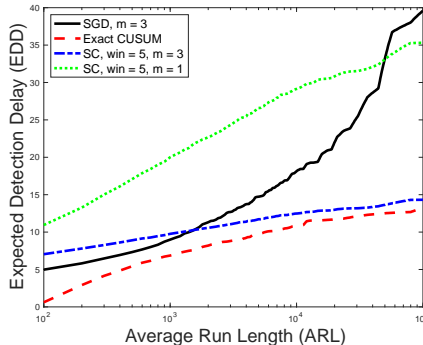


Figure 5: Comparison of the single eigenvector procedure and Exact-CUSUM procedure for switching membership problem. Community Size fixed to be 3. The total number of nodes in the network is set to be 50. Before the change, each community has a size 10, and after the change, each community size increases to 15 by absorbing nodes that do not belong to any community before change happens.

Synthetic data 3 is used to study the impact of network topology. We also explore the influence of the community density by assuming that for community i , the probability of forming an edge within the community is p_i . Then by changing the value of p_i under an emergence community scenario, the density of the community can change. From Figure 6 we see that a denser community structure after the change leads to a more accurate detection. However, we can also observe from the drastically decreasing curve that the detection can be performed more accurately if the community density $p_i \geq 0.4$. This provides an approach to discovering a community through the Spectral CUSUM method. In addition, we can see that the detection power increases with a larger m and the increase of community density. This result is consistent with our intuition since we can always collect more useful information when $m \leq k$, and the denser the community is, the signal that reveals the structure would be much stronger, leading to quicker change detection.

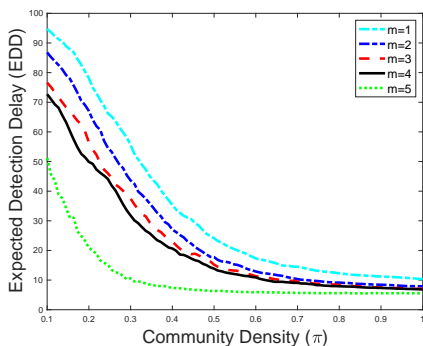


Figure 6: Relationship between the community density and EDD under different settings of the number of communities $m = \{1, 2, \dots, 5\}$. for emergence community problem. Smaller m leads to higher EDD and a larger community density π after the change would have also decreased the EDD.

6.3 Detecting changes of manifold structure

This section shows that our detection algorithm also works for detecting structural changes in the manifold. We first consider a one-dimensional manifold on two-dimensional rings. Before the change happens at time $t = 200$, the two rings are separately located, while after the change, there forms a bridge between the two rings, as shown in Figure 7.

We use the Isomap [46] to calculate the adjacency graph, which is sparse. Given the adjacency matrix, we set the threshold to eliminate all the edges whose distances run below the threshold. Thus, inside one community, any pair of members can be reached via a few steps. Using the Spectral-CUSUM, we show that in this case, we can detect the change quite quickly in figure 7(c).

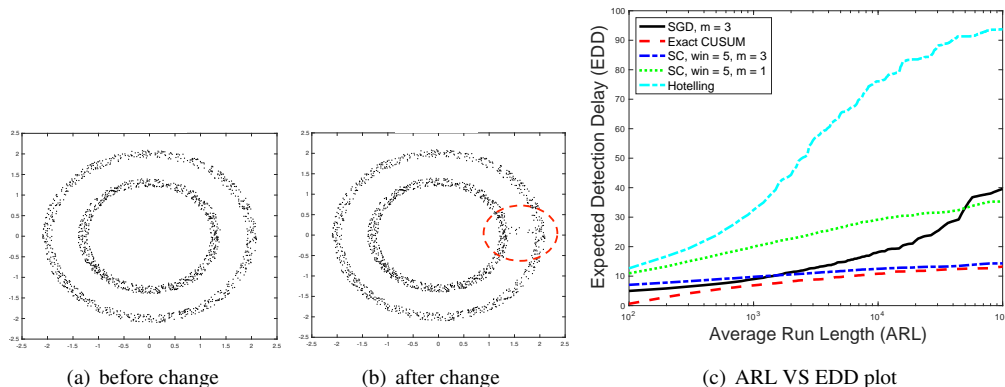


Figure 7: A case that two separate rings have some overlapping nodes by a bridge after the change: (a) Before the change, there are two rings structures which form two communities; (b) After the change, two communities remains the same, but some of their members join another community, leading to the overlapping of two communities. (c) The ARL VS EDD results show that Spectral-CUSUM when $m = 4$ outperforms other procedures under larger ARL, but SGD is better for smaller ARL.

Another classical manifold is Swiss Roll data [47], which is a two-dimensional structure lying in a three-dimensional space. The experiment is designed such that four Swiss rolls merge into two Swiss rolls after the change, as shown in Figure 6.3. We aim to use this to show that our method can deal with various data topological structure changes based on a choice of similarity measure. We see from the result that when m equals its potential community size, the performance is quite close to the optimal Exact-CUSUM.

6.4 Yellowstone seismic sensor network data

We further consider a seismic sensor network data set adapted from [48]. The sensors are placed in different locations to measure signals around the Old Faithful Geyser in the Yellowstone National Park. The total number of sensors is 19 in this case, but we removed four sensor signals since they failed to work during data collection. We then observe a sequence of sensor signals and translate each one into a dynamic cross-correlation graph. At the very beginning, the cross-correlation between each pair of sensors is low, which means they are not related. The emergence of community happens in the middle of the sequence. Such change will cause the infected sensors to generate similar signals, which lead to a higher correlation magnitude between them. In contrast, an unaffected sensor still generates random noises, thus having a low correlation with other sensors. Consequently, a community containing all the affected sensors emerges after the change happens. We visualize the correlation matrix for better understanding in Figure 9. In this case, the true changepoint time is roughly known, corresponding to the geyser eruption time.

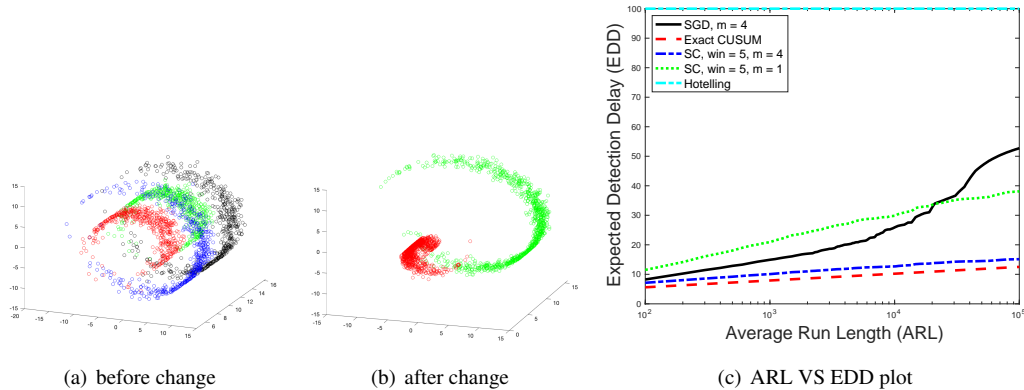


Figure 8: A case that four Swiss rolls merge into two communities after the change: (a) Before the change, there are four swiss roll structures which form four different communities; (b) After the change, two communities disappear and merge into the other communities. Note that in this experiment, Hotelling’s T -squared statistics cannot detect the change at all.

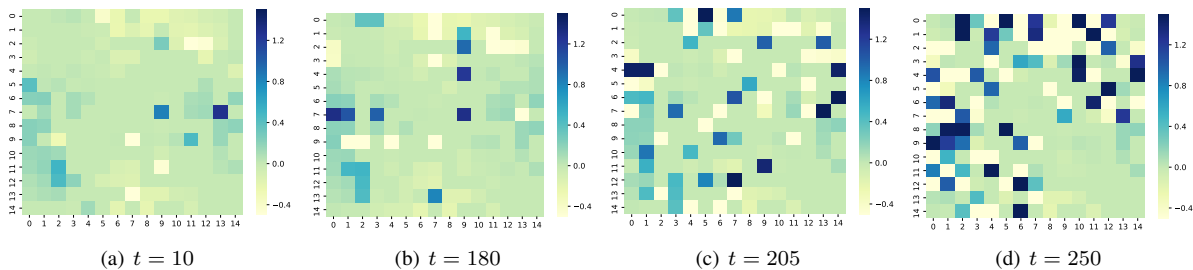


Figure 9: Correlation matrix for seismic sensors at different time $t = 10, 180, 205, 250$. We can see clearly from the above matrices that there’s a big change before and after $t = 200$, which is the ground-truth change-point in the seismic network, causing an emergence community scenario.

We apply our Spectral-CUSUM procedure to the dataset with choices of different potential community sizes m . Figure 10 (a) shows the sensor locations and the results of detection statistics using Spectral-CUSUM procedure are shown in Figure 10 (b). It can be seen clearly that setting potential community size $m \geq 4$ gives better performance on detecting change at around $t = 200$, which corresponds to a geyser eruption time – treated as a true change-point time. The result shows that the event can be detected without false alarms when $m \geq 4$, which reveals that this seismic network’s true underlying community size is about 4. The detection delay is shown in Table 1. This shows that our detection statistics can be useful when the underlying graph structure is unknown.

Table 1: Detection delays under different # communities (m) for seismic data.

| # communities (m) | 1 | 2 | 3 | 4 | 5 | 6 | 7 | 8 | 9 |
|-----------------------|----|----|----|---|---|---|---|---|---|
| Detection Delay | 23 | 20 | 17 | 4 | 3 | 3 | 2 | 2 | 2 |

In addition, we compare our Spectral-CUSUM with other methods on this real data. We can see from Figure 11 that Spectral-CUSUM and SGD have the most obvious abrupt change around the true change-point time 200. However, vectorized GLR and Hotelling’s T -squared statistics can not detect such a change.

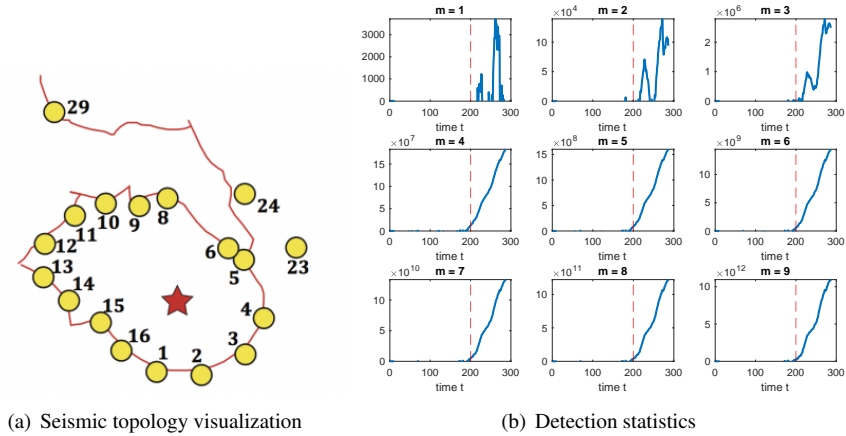


Figure 10: The topology of seismic sensors and detection statistics for sequential seismic data with an outburst of community structure changes. In (a), the total number of 19 seismic sensors roughly forms a circle, and signals can be observed on each sensor [49]. Thus the community would be formulated when an earthquake happens, making several sensors correlated. In (b), we applied our Spectral-CUSUM statistics on sensor signals, and we know the ground-truth earthquake happens at time 200. The results demonstrate the ability of the algorithm to detect such change very quickly.

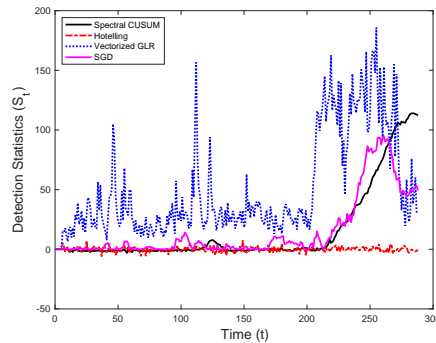


Figure 11: Comparison of our Spectral-CUSUM procedure with other baseline methods, including Hotelling's statistics, SGD and vectorized GLR.

7 Conclusion

We present a novel Spectral-CUSUM procedure for detecting underlying community changes through noisy observations. We provide the first-order asymptotic optimality of Spectral-CUSUM under the optimal choice of parameters. We also present an efficient online computation procedure to evaluate the Spectral-CUSUM statistic without remembering all data based on subspace tracking. Experimental results on both synthetic and real-world data demonstrate the superior performance of our procedure compared with alternative methods.

References

- [1] M. Faulkner, M. Olson, R. Chandy, J. Krause, K. M. Chandy, and A. Krause, "The next big one: Detecting earthquakes and other rare events from community-based sensors," in *Proceedings of the 10th ACM/IEEE Inter-*

- national Conference on Information Processing in Sensor Networks.* IEEE, 2011, pp. 13–24.
- [2] E. Ahmed, A. Clark, and G. Mohay, “A novel sliding window based change detection algorithm for asymmetric traffic,” in *2008 IFIP International Conference on Network and Parallel Computing.* IEEE, 2008, pp. 168–175.
- [3] M. Berger, L. M. Seversky, and D. S. Brown, “Classifying swarm behavior via compressive subspace learning,” in *2016 IEEE International Conference on Robotics and Automation (ICRA).* IEEE, 2016, pp. 5328–5335.
- [4] P. Basuchowdhuri, S. Sikdar, V. Nagarajan, K. Mishra, S. Gupta, and S. Majumder, “Fast detection of community structures using graph traversal in social networks,” *Knowledge and Information Systems*, vol. 59, no. 1, pp. 1–31, 2019.
- [5] H. Keshavarz, C. Scott, and X. Nguyen, “Optimal change point detection in gaussian processes,” *Journal of Statistical Planning and Inference*, vol. 193, pp. 151–178, 2018.
- [6] C. E. Johnson, A. Lindh, and B. Hirshorn, “Robust regional phase association,” 1997.
- [7] D. Vere-Jones, “Stochastic models for earthquake occurrence,” *Journal of the Royal Statistical Society: Series B (Methodological)*, vol. 32, no. 1, pp. 1–45, 1970.
- [8] T. Omi, Y. Ogata, Y. Hirata, and K. Aihara, “Forecasting large aftershocks within one day after the main shock,” *Scientific reports*, vol. 3, no. 1, pp. 1–7, 2013.
- [9] H.-H. Huang, F.-C. Lin, B. Schmandt, J. Farrell, R. B. Smith, and V. C. Tsai, “The yellowstone magmatic system from the mantle plume to the upper crust,” *Science*, vol. 348, no. 6236, pp. 773–776, 2015.
- [10] L. Peel and A. Clauset, “Detecting change points in the large-scale structure of evolving networks,” in *Twenty-Ninth AAAI Conference on Artificial Intelligence*, 2015.
- [11] N. Du, B. Wu, X. Pei, B. Wang, and L. Xu, “Community detection in large-scale social networks,” in *Proceedings of the 9th WebKDD and 1st SNA-KDD 2007 workshop on Web mining and social network analysis*, 2007, pp. 16–25.
- [12] A. Talwalkar, S. Kumar, and H. Rowley, “Large-scale manifold learning,” in *2008 IEEE Conference on Computer Vision and Pattern Recognition.* IEEE, 2008, pp. 1–8.
- [13] E. Abbe, “Community detection and stochastic block models: recent developments,” *The Journal of Machine Learning Research*, vol. 18, no. 1, pp. 6446–6531, 2017.
- [14] M. Fiedler, “Algebraic connectivity of graphs,” *Czechoslovak mathematical journal*, vol. 23, no. 2, pp. 298–305, 1973.
- [15] A. Pothen, H. D. Simon, and K.-P. Liou, “Partitioning sparse matrices with eigenvectors of graphs,” *SIAM journal on matrix analysis and applications*, vol. 11, no. 3, pp. 430–452, 1990.
- [16] S. Fortunato, “Community detection in graphs,” *Physics reports*, vol. 486, no. 3-5, pp. 75–174, 2010.
- [17] B. W. Kernighan and S. Lin, “An efficient heuristic procedure for partitioning graphs,” *Bell system technical journal*, vol. 49, no. 2, pp. 291–307, 1970.
- [18] C. Pizzuti, “Ga-net: A genetic algorithm for community detection in social networks,” in *International conference on parallel problem solving from nature.* Springer, 2008, pp. 1081–1090.

- [19] Y. Wang, A. Chakrabarti, D. Sivakoff, and S. Parthasarathy, “Fast change point detection on dynamic social networks,” *arXiv preprint arXiv:1705.07325*, 2017.
- [20] D. Eswaran, C. Faloutsos, S. Guha, and N. Mishra, “Spotlight: Detecting anomalies in streaming graphs,” in *Proceedings of the 24th ACM SIGKDD International Conference on Knowledge Discovery & Data Mining*, 2018, pp. 1378–1386.
- [21] S. Huang, Y. Hitti, G. Rabusseau, and R. Rabbany, “Laplacian change point detection for dynamic graphs,” in *Proceedings of the 26th ACM SIGKDD International Conference on Knowledge Discovery & Data Mining*, 2020, pp. 349–358.
- [22] I. U. Hewapathirana, D. Lee, E. Moltchanova, and J. McLeod, “Change detection in noisy dynamic networks: a spectral embedding approach,” *Social Network Analysis and Mining*, vol. 10, no. 1, pp. 1–22, 2020.
- [23] M. Yuan and Y. Lin, “Model selection and estimation in the gaussian graphical model,” *Biometrika*, vol. 94, no. 1, pp. 19–35, 2007.
- [24] H. Liu and L. Wang, “Tiger: A tuning-insensitive approach for optimally estimating gaussian graphical models,” *Electronic Journal of Statistics*, vol. 11, no. 1, pp. 241–294, 2017.
- [25] H. Keshavarz, G. Michailidis, and Y. Atchadé, “Sequential change-point detection in high-dimensional gaussian graphical models,” *Journal of machine learning research*, vol. 21, no. 82, 2020.
- [26] Y. Xie, J. Huang, and R. Willett, “Change-point detection for high-dimensional time series with missing data,” *IEEE Journal of Selected Topics in Signal Processing*, vol. 7, no. 1, pp. 12–27, 2012.
- [27] J. Yang, J. McAuley, and J. Leskovec, “Community detection in networks with node attributes,” in *2013 IEEE 13th international conference on data mining*. IEEE, 2013, pp. 1151–1156.
- [28] E. S. Page, “Continuous inspection schemes,” *Biometrika*, vol. 41, no. 1/2, pp. 100–115, 1954.
- [29] G. Lorden, “Procedures for reacting to a change in distribution,” *The Annals of Mathematical Statistics*, vol. 42, no. 6, pp. 1897–1908, 1971.
- [30] G. V. Moustakides, “Optimal stopping times for detecting changes in distributions,” *The Annals of Statistics*, vol. 14, no. 4, pp. 1379–1387, 1986.
- [31] T. Oskiper and H. V. Poor, “Quickest detection of a random signal in background noise using a sensor array,” *EURASIP Journal on Advances in Signal Processing*, vol. 2005, no. 1, p. 360150, 2005.
- [32] D. Egea-Roca, G. Seco-Granados, and J. A. López-Salcedo, “Comprehensive overview of quickest detection theory and its application to gnss threat detection,” *Gyroscopy and Navigation*, vol. 8, no. 1, pp. 1–14, 2017.
- [33] G. V. M. Liyan Xie and Y. Xie, “Window-limited CUSUM for sequential change detection,” *arXiv preprint arXiv:2206.06777*, 2022.
- [34] L. Xie, G. V. Moustakides, and Y. Xie, “First-order optimal sequential subspace change-point detection,” in *2018 IEEE Global Conference on Signal and Information Processing (GlobalSIP)*. IEEE, 2018, pp. 111–115.
- [35] L. Xie, Y. Xie, and G. V. Moustakides, “Sequential subspace change point detection,” *Sequential Analysis*, vol. 39, no. 3, pp. 307–335, 2020.

- [36] T. W. Anderson, “Asymptotic theory for principal component analysis,” *Annals of Mathematical Statistics*, vol. 34, no. 1, pp. 122–148, 1963.
- [37] D. Siegmund, *Sequential analysis: tests and confidence intervals*. Springer Science & Business Media, 2013.
- [38] L. Balzano, R. Nowak, and B. Recht, “Online identification and tracking of subspaces from highly incomplete information,” in *2010 48th Annual allerton conference on communication, control, and computing (Allerton)*. IEEE, 2010, pp. 704–711.
- [39] U. Von Luxburg, “A tutorial on spectral clustering,” *Statistics and computing*, vol. 17, no. 4, pp. 395–416, 2007.
- [40] A. Edelman, T. A. Arias, and S. T. Smith, “The geometry of algorithms with orthogonality constraints,” *SIAM journal on Matrix Analysis and Applications*, vol. 20, no. 2, pp. 303–353, 1998.
- [41] K. B. Petersen and M. S. Pedersen, “The matrix cookbook,” *Technical University of Denmark*, vol. 7, no. 15, p. 510, 2008.
- [42] B. Sarwar, G. Karypis, J. Konstan, and J. Riedl, “Incremental singular value decomposition algorithms for highly scalable recommender systems,” in *Fifth international conference on computer and information science*, vol. 1, no. 012002. Citeseer, 2002, pp. 27–8.
- [43] R. L. Bishop and R. J. Crittenden, *Geometry of manifolds*. Academic press, 2011.
- [44] T. L. Lai, “Information bounds and quick detection of parameter changes in stochastic systems,” *IEEE Transactions on Information Theory*, vol. 44, no. 7, pp. 2917–2929, 1998.
- [45] H. Hotelling, “The generalization of student’s ratio,” in *Breakthroughs in statistics*. Springer, 1992, pp. 54–65.
- [46] M. Balasubramanian and E. L. Schwartz, “The isomap algorithm and topological stability,” *Science*, vol. 295, no. 5552, pp. 7–7, 2002.
- [47] C. Moolenbeek and E. Ruitenbergh, “The ‘swiss roll’: a simple technique for histological studies of the rodent intestine,” *Laboratory animals*, vol. 15, no. 1, pp. 57–60, 1981.
- [48] X. He, Y. Xie, S.-M. Wu, and F.-C. Lin, “Sequential graph scanning statistic for change-point detection,” in *2018 52nd Asilomar Conference on Signals, Systems, and Computers*. IEEE, 2018, pp. 1317–1321.
- [49] S.-M. Wu, K. M. Ward, J. Farrell, F.-C. Lin, M. Karplus, and R. B. Smith, “Anatomy of old faithful from subsurface seismic imaging of the yellowstone upper geyser basin,” *Geophysical Research Letters*, vol. 44, no. 20, pp. 10–240, 2017.

Proof of Lemma 1. Since \widehat{A}_t is estimated using data from $t + 1$ to $t + w$, it is *independent* from v_t . This independence property allows for the straightforward computation of the two expectations in Lemma 1 and contributes towards the proper selection of drift d . Note that under the pre-change distribution we can write:

$$\begin{aligned}
& \mathbb{E}_\infty[v_t^\top \widehat{A}_t \widehat{A}_t^\top v_t] \\
&= \mathbb{E}_\infty[v_t^\top \widehat{U}_t \widehat{\Lambda}_t^{-1} \widehat{U}_t^\top v_t] = \mathbb{E}_\infty[v_t^\top (\sum_{i=1}^m \frac{1}{\widehat{\lambda}_{ti}} \widehat{u}_{ti} \widehat{u}_{ti}^\top) v_t] \\
&= \sum_{i=1}^m \mathbb{E}_\infty[\frac{1}{\widehat{\lambda}_{ti}} (\widehat{u}_{ti}^\top v_t)^2] = \sum_{i=1}^m \mathbb{E}_\infty[\frac{1}{\widehat{\lambda}_{ti}} \widehat{u}_{ti}^\top \mathbb{E}_\infty[v_t v_t^\top] \widehat{u}_{ti}] \\
&= \frac{1}{\sigma^2} \sum_{i=1}^m \mathbb{E}_\infty[\frac{1}{\widehat{\lambda}_{ti}} \widehat{u}_{ti}^\top \widehat{u}_{ti}] = \frac{1}{\sigma^2} \sum_{i=1}^m \mathbb{E}_\infty[\frac{1}{\widehat{\lambda}_{ti}}].
\end{aligned}$$

Note that under the pre-change measure, the estimated \widehat{U}_t and $\widehat{\Lambda}_t$ are eigenvectors and eigenvalues for the sample covariance matrix constructed by samples generated from zeros-mean and covariance matrix $(1/\sigma^2)I$. Following the discussions above we have:

$$\mathbb{E}_\infty[v_t^\top \widehat{A}_t \widehat{A}_t^\top v_t] \approx m. \quad (28)$$

Similarly, we can derive the results for post-change distribution:

$$\begin{aligned}
& \mathbb{E}_0[v_t^\top \widehat{A}_t \widehat{A}_t^\top v_t] \\
&= \mathbb{E}_0[v_t^\top \widehat{U}_t \Lambda_t^{-1} \widehat{U}_t^\top v_t] = \mathbb{E}_0[v_t^\top (\sum_{i=1}^m \frac{1}{\widehat{\lambda}_{ti}} \widehat{u}_{ti} \widehat{u}_{ti}^\top) v_t] \\
&= \sum_{i=1}^m \mathbb{E}_0[\frac{1}{\widehat{\lambda}_{ti}} (\widehat{u}_{ti}^\top v_t)^2] = \sum_{i=1}^m \mathbb{E}_0[\frac{1}{\widehat{\lambda}_{ti}} \widehat{u}_{ti}^\top \mathbb{E}_0[v_t v_t^\top] \widehat{u}_{ti}] \\
&= \sum_{i=1}^m \sum_{j=1}^n \mathbb{E}_0[\frac{\lambda_j}{\widehat{\lambda}_{ti}} (\widehat{u}_{ti}^\top u_j)^2],
\end{aligned}$$

where $\lambda_1, \dots, \lambda_n$ are the eigenvalues of the covariance matrix $(AA^\top + \sigma^2 I)^{-1}$. As stated in Theorem 1, the estimated eigenvalue and eigenvector from the sample covariance matrix is independent, and Theorem 1 characterizes the estimation error $e_i = \widehat{\varphi}_{ti} - u_i$. Since the estimated eigenvector is normalized to be unit-norm, we have the following:

$$\widehat{u}_{it} = \frac{\widehat{\varphi}_{ti}}{\|\widehat{\varphi}_{ti}\|} = \frac{u_i + e_i}{\|u_i + e_i\|}.$$

First of all, due to the orthogonality of different eigenvectors, we have:

$$\sum_{i=1}^m \sum_{j=1}^n \mathbb{E}_0[\frac{\lambda_j}{\widehat{\lambda}_{ti}} (\widehat{u}_{ti}^\top u_j)^2] = \sum_{i=1}^m \mathbb{E}_0[\frac{\lambda_i}{\widehat{\lambda}_{ti}} (\widehat{u}_{ti}^\top u_i)^2],$$

where $u_i, i = 1, \dots, m$, are the eigenvectors corresponding to the smallest m eigenvalues of the true covariance matrix.

Combining these together, we have

$$\begin{aligned}
\mathbb{E}_0[v_t^\top \widehat{A}_t \widehat{A}_t^\top v_t] &= \sum_{i=1}^m \mathbb{E}_0 \left[\frac{\lambda_i}{\lambda_{ti}} (\widehat{u}_{ti}^\top u_i)^2 \right] = \sum_{i=1}^m \mathbb{E}_0 \left[\frac{(\|u_i\|^2 + e_i^\top u_i)^2}{\|u_i + e_i\|^2} \right] \\
&= \sum_{i=1}^m \mathbb{E}_0 \left[\frac{(1 + e_i^\top u_i)^2}{1 + \|e_i\|^2} \right] = \sum_{i=1}^m \mathbb{E}_0 \left[\frac{1}{1 + \|e_i\|^2} \right] \\
&= \sum_{i=1}^m \left\{ 1 - \mathbb{E}_0[\|e_i\|^2] + \mathbb{E}_0 \left[\frac{\|e_i\|^4}{1 + \|e_i\|^2} \right] \right\}.
\end{aligned}$$

For the two expectations above, using Gaussian approximation from Theorem 1, we have

$$\mathbb{E}_0[\|e_i\|^2] = \frac{1}{w} \sum_{k=1, k \neq i}^m \frac{\lambda_i \lambda_k}{(\lambda_i - \lambda_k)^2} = \frac{B_i}{w},$$

and

$$\mathbb{E}_0 \left[\frac{\|e_i\|^4}{1 + \|e_i\|^2} \right] \leq \mathbb{E}_0[\|e_i\|^4] \leq \frac{3}{w^2} \left(\sum_{k=1, k \neq i}^m \frac{\lambda_i \lambda_k}{(\lambda_i - \lambda_k)^2} \right)^2 = \frac{3B_i^2}{w^2}.$$

Therefore, we get the desired post-change expectation:

$$\mathbb{E}_0[v_t^\top \widehat{A}_t \widehat{A}_t^\top v_t] \leq \sum_{i=1}^m \left(1 - \frac{B_i}{w} + \frac{3B_i^2}{w^2} \right).$$

If we ignore the higher-order term, the above expectation can also be written as

$$\mathbb{E}_0[v_t^\top \widehat{A}_t \widehat{A}_t^\top v_t] = \sum_{i=1}^m (1 - B_i/w) + o(1/w).$$

□

Proof of Lemma 2. Following previous results, we define $\psi(w) = \mathbb{E}_0(\mathcal{T}_C)$ in (19) as a function of w and try to find the w^* that minimizes $\psi(w)$. First we have:

$$D = \sum_{i=1}^m \left(1 - \frac{B_i}{w} + \frac{3B_i^2}{w^2} \right) = m - \frac{\sum_{i=1}^m B_i}{w} + \frac{3 \sum_{i=1}^m B_i^2}{w^2}.$$

Thus we can re-write $\psi(w)$ as:

$$\psi(w) = w + \frac{2 \log \gamma}{-\sum B_i/w + 3 \sum B_i^2/w^2 - m \log(1 - \frac{\sum B_i}{mw} + \frac{3 \sum B_i^2}{mw^2})}.$$

If we use the approximation that $\log(1+x) \approx x$ around 0 on the log part in the denominator, then it would become 0, which is not computable. Thus we need to derive a tighter approximation for the denominator. Note that

$$\mathbb{E}_0(v_t^\top A A^\top v_t) = \sum_{i=1}^m \frac{\lambda_i}{\sigma^2 + \lambda_i} \neq m,$$

and we estimate A_t^\top using \hat{U}_t and $\hat{\Lambda}'_t$ where $\hat{\lambda}'_{ti} = 1/\hat{\lambda}_{ti} - \sigma^2$ because sample eigenvalue $\hat{\lambda}_{ti} \approx 1/(\sigma^2 + |C_i|)$ and then $1/\hat{\lambda}'_{ti} - \sigma^2 \approx |C_i| = \lambda_i$. Let

$$\begin{aligned} D' &= \mathbb{E}'_0(v_t^\top AA^\top v_t) \\ &= \sum_{i=1}^m \mathbb{E}_0 \left(\frac{\hat{\lambda}'_{ti}}{\lambda_i + \sigma^2} (\hat{u}_{ti}^\top u_i)^2 \right) \\ &= \sum_{i=1}^m \frac{\lambda_i}{\lambda_i + \sigma^2} \left[1 - \mathbb{E}_0(\|e_i\|^2) + \mathbb{E}_0 \left[\frac{\|e_i\|^4}{1 + \|e_i\|^2} \right] \right] \\ &\approx \sum_{i=1}^m \frac{\lambda_i}{\lambda_i + \sigma^2} \left(1 - \frac{B_i}{w} + \frac{3B_i^2}{w^2} \right). \end{aligned}$$

Using D' instead of D gives us the expression for the EDD as:

$$\psi(w) = \frac{2 \log \gamma}{D' - m + m \log(m/D')} + w.$$

Let

$$\delta D = m - \sum_{i=1}^m \frac{\lambda_i}{\lambda_i + \sigma^2},$$

so that δD is close to 0 when σ^2 is small. Then we have:

$$D' = m - \delta D - \sum_{i=1}^m \frac{\lambda_i B_i}{\sigma^2 + \lambda_i} \frac{1}{w} + \sum_{i=1}^m \frac{3B_i^2 \lambda_i}{\sigma^2 + \lambda^2} \frac{1}{w^2}.$$

Let

$$\begin{aligned} B'_i &= \frac{\lambda_i B_i}{\sigma^2 + \lambda_i}; \\ C'_i &= \frac{3B_i^2 \lambda_i}{\sigma^2 + \lambda^2}. \end{aligned}$$

We have

$$D' = m - \delta D - \frac{\sum B'_i}{w} + \frac{\sum C'_i}{w^2}.$$

Then

$$\begin{aligned} \psi(w) &= w + \\ &\frac{2 \log \gamma}{-\delta D - \frac{\sum B'_i}{w} + \frac{\sum C'_i}{w^2} - m \log \left(1 - \frac{\delta D}{m} - \frac{\sum B'_i}{mw} + \frac{\sum C'_i}{mw^2} \right)}. \end{aligned}$$

Note that

$$\begin{aligned} &1 - \frac{\delta D}{m} - \frac{\sum B'_i}{mw} + \frac{\sum C'_i}{mw^2} \\ &= \left(1 - \frac{\delta D}{m} \right) \left(1 - \frac{\sum B'_i}{(1 - \delta D/m)mw} + \frac{\sum C'_i}{(1 - \delta D/m)mw^2} \right). \end{aligned}$$

Using $\log(1 - x) \approx -x$, we have

$$\begin{aligned} & \log \left(1 - \frac{\sum B'_i}{(1 - \delta D/m)mw} + \frac{\sum C'_i}{(1 - \delta D/m)mw^2} \right) \\ & \approx -\frac{\sum B'_i}{(1 - \delta D/m)mw} + \frac{\sum C'_i}{(1 - \delta D/m)mw^2}. \end{aligned}$$

Substitute into $\psi(w)$ and note that the denominator will be dominated by the term $= -\delta D - m \log(1 - \delta D/m)$. Let the first-order derivative of $\psi(w)$ equal to 0 and simply ignore $O(w^2)$ term, it can be seen clearly that when $\psi'(w^*) = 0$ we get the minimum value for $\psi(w)$. Thus we have:

$$\begin{aligned} w^* &= \frac{\sqrt{2 \log \gamma \left(\frac{1}{1 - \delta D/m} - 1 \right) (\sum B'_i)}}{-\delta D - m \log(1 - \delta D/m)} \\ &= \frac{\sqrt{2 \log \gamma \left(\frac{1}{1 - \delta D/m} - 1 \right) (\sum \frac{\lambda_i B_i}{\sigma^2 + \lambda_i})}}{-m + \sum_{i=1}^m \frac{\lambda_i}{\sigma^2 + \lambda_i} - m \log \left(\sum_{i=1}^m \frac{\lambda_i}{m\sigma^2 + m\lambda_i} \right)}. \end{aligned}$$

Note that the denominator is always positive since $\log(1 + x) \leq x$ for all $x > -1$. □